
Transcoder-based Circuit Analysis for Interpretable Single-Cell Foundation Models

Sosuke Hosokawa

The University of Tokyo
Tokyo, Japan

hosososuke0421@g.ecc.u-tokyo.ac.jp

Toshiharu Kawakami

The University of Tokyo Hospital
Tokyo, Japan

kawakami-toshinaru555@g.ecc.u-tokyo.ac.jp

Satoshi Kodera

The University of Tokyo Hospital
Tokyo, Japan

koderasatoshi@gmail.com

Masamichi Ito

The University of Tokyo Hospital
Tokyo, Japan

mitou.tky@gmail.com

Norihiko Takeda

The University of Tokyo Hospital
Tokyo, Japan

ntakeda-tky@g.ecc.u-tokyo.ac.jp

Abstract

Single-cell foundation models (scFMs) have demonstrated state-of-the-art performance on various tasks, such as cell-type annotation and perturbation response prediction, by learning gene regulatory networks from large-scale transcriptome data. However, a significant challenge remains: the decision-making processes of these models are less interpretable compared to traditional methods like differential gene expression analysis. Recently, transcoders have emerged as a promising approach for extracting interpretable decision circuits from large language models (LLMs). In this work, we train a transcoder on the cell2sentence (C2S) model, a state-of-the-art scFM. By leveraging the trained transcoder, we extract internal decision-making circuits from the C2S model. We demonstrate that the discovered circuits correspond to real-world biological mechanisms, confirming the potential of transcoders to uncover biologically plausible pathways within complex single-cell models.

1 Introduction

In recent years, single-cell foundation models (scFMs) such as cell2sentence (C2S) [12] and Geneformer [15] have garnered significant attention in the field of computational biology. These models adapt techniques from large language models (LLMs) in natural language processing, combining pre-training on large-scale transcriptome data corpora to learn general gene-gene relationships with task-specific fine-tuning on smaller datasets [15, 4]. While these models have achieved state-of-the-art performance on various single-cell analysis tasks including cell-type annotation and cellular response prediction, their low interpretability, stemming from the inherent nature of neural network algorithms, remains a significant challenge. This is particularly crucial in single-cell analysis models, where biological interpretation of model predictions is essential, making improved interpretability in scFMs an urgent priority.

A major goal in efforts to elucidate the internal mechanisms of large-scale models like LLMs and scFMs includes identifying internal circuits: the combinations of features that determine model behavior (circuit tracing) [6, 8]. In single-cell analysis models, discovered internal circuits could potentially lead to new discoveries when connected with biological insights. This pursuit of understanding model internal mechanisms falls under the research field of mechanistic interpretability, which has recently attracted considerable attention.

In the domain of natural language processing, mechanistic interpretability of LLMs has emerged as a major research topic, with various methods being proposed. Among these, sparse autoencoders (SAEs) [9] and their variant, transcoders [6], have gained attention as methods that can resolve the "polysemanticity" within LLMs and transform internal representations into interpretable features. Transcoders, in particular, have been shown to extract input-invariant and highly interpretable features by training neural networks with wide, sparsely activated intermediate layers that replace MLP layers, enabling the extraction of model internal circuits.

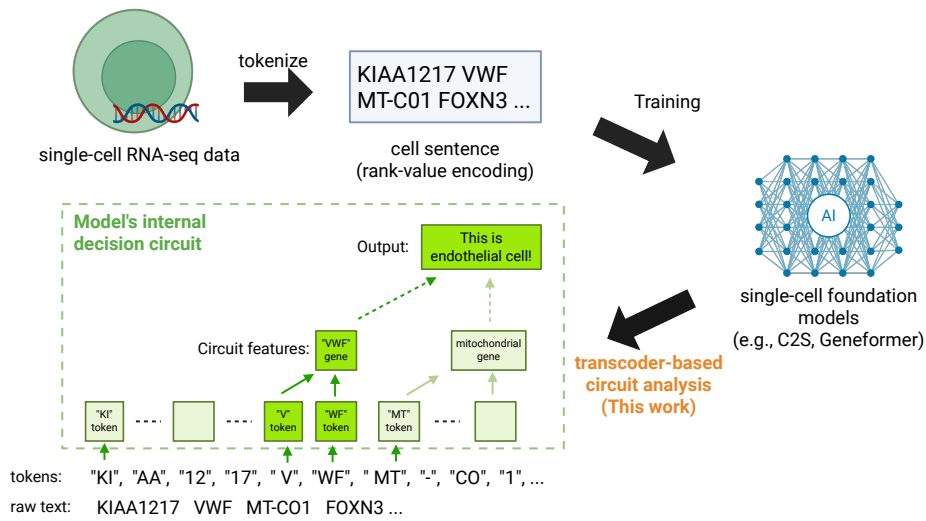


Figure 1: Pipeline for transcoder-based circuit tracing in scFMs. We train a transcoder on each MLP and attribute across features and attention to recover a sparse computational subgraph (circuit) that underlies cell-type predictions. The recovered features align with known endothelial biology (e.g., VWF, PTPRB, SPARCL1).

In this work, we apply transcoders to the C2S model, a state-of-the-art scFM, to extract its internal circuits and biologically interpret the circuit components (Figure 1). Our contributions are summarized as follows:

- We apply transcoders to scFMs (for the first time to our knowledge), demonstrating their effectiveness for mechanistic interpretability of scFMs.
- We establish correspondences between extracted circuit components and biological knowledge, showing that biologically plausible circuits can be extracted.
- We discuss challenges and future directions when applying transcoders to scFMs for mechanistic interpretability.

The remainder of this paper is organized as follows. We first explain the background methods of scFMs and transcoders along with their use for circuit analysis. We then discuss case studies of experiments applying transcoders to the C2S model. Subsequently, we summarize related work on interpretability in single-cell analysis models, and finally present conclusions and future perspectives.

2 Single-cell Foundation Models

Single-cell foundation models (scFMs) are transformer-based models pre-trained on large-scale transcriptome data. These models process input by ranking genes within each cell based on their expression levels and other factors, then arranging genes in rank order to form gene sequences. Prominent examples include Geneformer, scGPT, and cell2sentence (C2S).

ScFMs exhibit several architectural variations:

- **Architecture type:** Models can be either encoder-based or decoder-based.
- **Tokenization method:** Some models tokenize at the gene level, while others leverage natural language tokenizers to process gene sequences represented as natural language strings.
- **Gene ranking methods:** Different approaches exist for ranking genes [15, 12], which represents a unique challenge specific to scFMs.

In this work, we focus on the C2S model, which employs a decoder-based architecture and utilizes natural language tokenization. C2S leverages the Pythia [1] architecture and tokenizer, pre-trained on 57 million human and mouse cells from scRNA-seq data, along with biological literature abstracts [12]. This approach enables the model to capture both gene expression patterns and broader biological knowledge from scientific texts.

3 Transcoders and Circuit Tracing

3.1 The Need for Transcoders: Resolving Polysemanticity

Understanding the internal representations of LLMs faces a fundamental challenge known as *polysemanticity*: the phenomenon where individual neurons or weights simultaneously encode multiple distinct concepts or functions [7]. For instance, a single neuron might strongly respond to both Japanese city names and gene names. This polysemanticity makes it difficult to disentangle and understand which parts of the weight matrices represent specific concepts through direct observation.

To resolve or mitigate polysemanticity and reconstruct the internals of large models into human-interpretable units, methods such as sparse autoencoders (SAEs) and their variant, transcoders, have proven effective [9, 6].

3.2 Sparse Autoencoders and Transcoders

3.2.1 Sparse Autoencoders (SAE)

SAEs consist of an encoder that transforms an input vector $\mathbf{x} \in \mathbb{R}^d$ into a higher-dimensional activation vector $\mathbf{z} \in \mathbb{R}_{\geq 0}^l$ (where $l > d$), and a decoder that reconstructs the original dimension:

$$\mathbf{z} = \text{ReLU}(\mathbf{W}_{\text{enc}}\mathbf{x} + \mathbf{b}_{\text{enc}}) \tag{1}$$

$$\hat{\mathbf{x}} = \mathbf{W}_{\text{dec}}\mathbf{z} + \mathbf{b}_{\text{dec}} \tag{2}$$

Typical SAEs use the same LLM hidden state for both encoder input and decoder output, and are trained to minimize the following loss function:

$$\mathcal{L} = \|\hat{\mathbf{x}} - \mathbf{x}\|_2^2 + \lambda\|\mathbf{z}\|_1 \tag{3}$$

where the first term represents reconstruction error, the second term is a sparsity penalty that encourages sparse activations, and λ is a hyperparameter controlling the L1 weight.

3.2.2 Transcoders

Transcoders are a variant of SAEs that learn on the input and output of each transformer layer’s MLP rather than on the same hidden state:

$$\mathcal{L} = \|\hat{\mathbf{x}} - \text{MLP}(\mathbf{x})\|_2^2 + \lambda\|\mathbf{z}\|_1 \tag{4}$$

This formulation enables transcoders to approximate the transformer’s MLP, decomposing MLP neurons into interpretable components.

3.2.3 Key Differences between SAEs and Transcoders

While standard SAEs are trained to reproduce hidden states and extract input-dependent features, transcoders approximate specific modules within transformers (the MLPs) and thus extract input-invariant features. For explaining general model behavior, input-invariant features are preferable; therefore, transcoders are better suited for extracting circuits within transformers.

3.3 Circuit Tracing with Transcoders

Recent work has proposed methods for tracing circuits within LLMs using transcoders. We outline the key components below.

3.3.1 Attribution Between Transcoder Feature Pairs

The contribution of transcoder feature i in layer l to feature j in layer l' is computed as:

$$z^{(l,i)}(x) \times (f_{\text{dec}}^{(l,i)} \cdot f_{\text{enc}}^{(l',j)}) \tag{5}$$

where $z^{(l,i)}(x)$ represents the input-dependent activation level, and the dot product $(f_{\text{dec}} \cdot f_{\text{enc}})$ is an input-independent fixed value. Here, $f_{\text{enc/dec}}^{(l,i)}$ denotes feature vector i of the transcoder encoder/decoder in layer l , corresponding to row vectors of \mathbf{W}_{enc} and column vectors of \mathbf{W}_{dec} respectively. This decomposition allows separate treatment of "input-independent general connections" and "input-specific importance."

3.3.2 Attribution Through Attention Heads

Inter-feature relationships propagate not only through MLPs within the same token but also from different tokens via attention heads. Through the OV matrices of attention heads [10], we can track which token's information contributes to specific features. Mathematically, by combining attention scores with OV matrices, we can compute how representations from source tokens contribute to downstream transcoder features.

3.3.3 Finding Computational Subgraphs

By iteratively applying the attribution calculations above, we can identify the primary computational paths that activate specific features [6]. The process involves:

1. Search for upstream features that strongly contribute to the target feature
2. Retain only top contributors and extend the paths
3. Iterate to obtain a set of important computational paths

Integrating these paths yields a sparse *computational subgraph* (circuit) that represents the model's internal decision-making process.

4 Experiments

4.1 Training Transcoder on C2S

4.1.1 Experimental Setup

We trained transcoders on each MLP layer of `vandijklab/C2S-Pythia-410m-cell-type-prediction` [17], a model from the C2S family from Hugging Face. For training data, we used the Heart Cell Atlas v2 [11] dataset, splitting it into 90% for training and 10% for validation.

4.1.2 Training Hyperparameters

The transcoder training was conducted with the following hyperparameters:

- Maximum learning rate: 1×10^{-4}

- Number of tokens per batch: 2048
- L1 coefficient: 1.4×10^{-4}
- Hidden dimension of transcoder: 8192 (expansion factor 8)
- Number of training tokens: 60 million

4.1.3 Model Validation

To validate the trained transcoders, we compared three models: the original model, a model with all MLPs replaced by transcoders, and a model with all MLPs removed. Table 1 shows the validation losses for each model configuration.

Model Configuration	Original	Transcoder	No MLP
Validation Loss	2.48	4.63	12.67

Table 1: Validation loss comparison across different model configurations.

While the transcoder-replaced model shows some degradation compared to the original model, it achieves substantially lower loss than the model with MLPs removed, confirming that the transcoders successfully capture significant MLP functionality.

Additionally, we computed the KL divergence between the logits of the modified models and the original model:

	KL(Original Transcoder)	KL(Original No MLP)
Mean	2.406	10.52

Table 2: KL divergence between original model and modified models.

The average number of activated transcoder features per token (L0 value) across layers is shown in Figure 2.

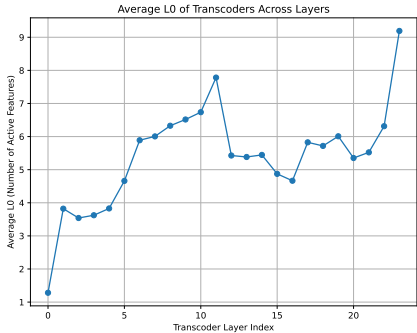


Figure 2: Average L0 values (number of active features per token) across transcoder layers.

4.2 Human Evaluation of Transcoder Features’ Interpretability

To evaluate the interpretability of learned transcoder features, we conducted a human evaluation study. We focused on transcoder features from layer 12, defining "live features" as those with $\log_{10} E(f) \geq -4$, where $E(f)$ represents the probability that feature f activates per token. Figure 3 shows the distribution of live features.

From these live features, we randomly selected 20 features for detailed interpretation. Features were analyzed by investigating which tokens activate them. A feature was classified as "gene-level interpretable" if it consistently activated on tokens corresponding to specific genes or gene families.

Our evaluation revealed that 7 out of 20 features (35%) were gene-level interpretable. Table 3 presents the detailed analysis of each feature.

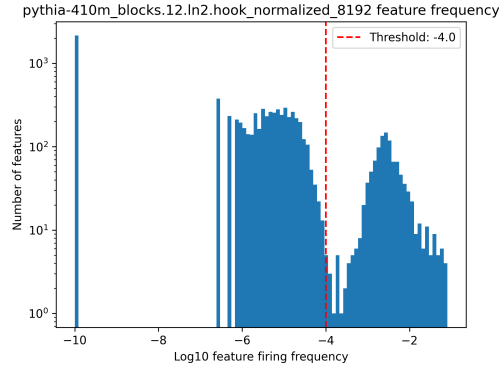


Figure 3: Distribution of live features in layer 12 transcoder with $\log_{10} E(f) \geq -4$.

Feature ID	$\log_{10} E(f)$	Activating Tokens	Gene-Level Interpretable
6027	-2.66	_PSD token in PSD3 gene	Yes
2123	-2.60	OL token in GOLGA4, GOLGA8A, GOLPH3	No
4942	-1.25	Trailing 2 token in genes	No
2459	-3.01	_Y tokens (non-specific)	No
7892	-2.50	_ME token in MEIS2, MEF2A	No
7125	-2.53	PN token in PTPN family genes	Yes
3266	-2.90	SH token in TSHZ2, TSHZ3	No
1702	-2.43	AM token in LAM* genes (LAMC1, LAMTOR4)	No
3546	-2.34	X token in YBX1, YBX3	Yes
4319	-2.96	AA token in HSP90AA1 gene	Yes
2709	-2.57	BL token in ABLIM1, ABL1, ABLIM3	No
1283	-1.71	20 token in ZBTB20 gene	No
5085	-2.60	NA token in GNA* genes (GNAI1, GNAI2, GNA14)	No
2271	-2.67	NK token in CSNK family genes	Yes
1980	-2.91	_NA token in NAALADL2, NAIP	No
2808	-2.53	OCK token in ROCK1, ROCK2	No
4619	-2.90	NN token in TNNI3, TNNC1	No
5951	-2.41	O token in FOXO family genes	Yes
4819	-2.31	SB token in WSB family genes	Yes
5280	-1.98	3 token in RPS3, RPS3A	No

Table 3: Human interpretation of randomly selected transcoder features from layer 12. Note: In token representations, underscore () denotes a space character.

4.3 Case Study: Interpreting Cell Type Classification

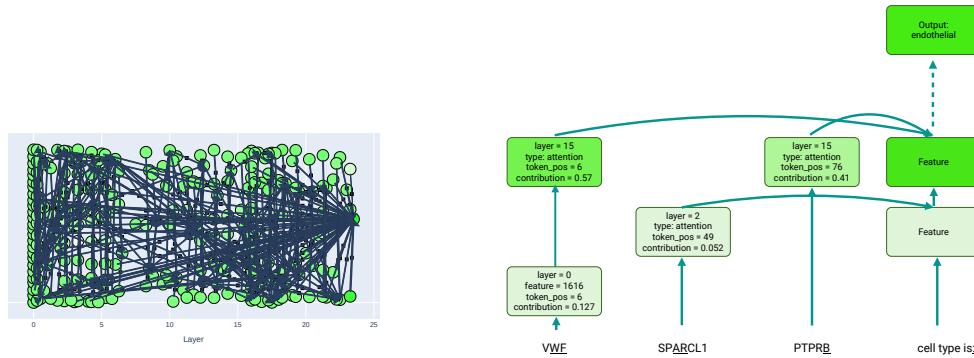
To demonstrate the practical application of circuit tracing in scFMs, we analyzed how the C2S model performs cell type classification. We extracted a cell labeled as endothelial cell from Heart Cell Atlas v2 and prepared the prompt shown in Figure ??.

KIAA1217 VWF MT-CO1 FOXN3 MT-CO2 ENG MGLL MT-ND4 MAGI1 MT-CO3 MT-CYB IQGAP1 SYNE1 CD36 RASAL2 SPARCL1 ST6GALNAC3 LINC00486 RAPGEF1 ID1 RBMS3 NFIB PTPRB LRMDA ARID2 MT-ATP6 SMAD2 ZBTB20 RGCC PLAA SLC48A1 TACC1 MECOM RB1 TSPAN14 FRMD4A AFDN ANO2 SHOC2 CDC42BPA RASGRF2 CCDC85A ESR2 SLC1A1 FRYL MALAT1 FAM241A DIAPH2 TSPAN15 LPAR6 HIF3A ITGA6 PARP14 NSD3 WNT2B FTX ART4 FBXW11 MTHFR AFF1 KHDRBS1 ZBTB46 ANKRD13C RDX SRSF11 ROCK2 SRSF10 BPTF GRB10 ATG4C AHCYL2 CFPD1 AC108449.1 NUTM2B-AS1 CNTNAP3B FAM214A LNX1 LRP5 MAP2K5 AL138828.1 SIPA1L3 UVRAG FLI1 GNAI3 EGFL7 ARL17B IL17RA ASAP1 ZFP36L1 PHLPP1 ASXL2 MT-ND1 NUTM2A-AS1 KIAA1671 LIFR FSD1L PRMT9 DIPK2B KIAA1328 TIMP3 CEP68 KIAA0100 KALRN PTPRM PPP3CC NR3C1 FBXL7 WDR60 ABLIM3 WWP1 ZNF761 LINC01060 ZNF274 TTC28 EPAS1 C6ORF89 B2M FOXN2 NRP1 SMIM17 VAV3 NCOA3 CCN2 GNAQ WNK1 GMDS ZBTB16 MPPED2.
The corresponding cell type is:

Figure 4: Prompt for cell type classification consisting of 128 genes ordered by C2S gene rank encoding.

This prompt consists of the top 128 genes arranged according to C2S's gene rank encoding (a cell sentence), followed by a query for cell type prediction. The C2S model (vandijklab/C2S-Pythia-410m-cell-type-prediction) successfully predicted "endothelial cell of artery" as the cell type.

We extracted circuits for features that strongly activated on the final token (":") in the last layer. Figure 5 shows an example circuit extracted for feature ID 3353, one of the most strongly activated features.



(a) Extracted circuit for feature 3353 activated during endothelial cell classification. The circuit shows the computational graph tracing back from the final prediction token.

(b) Simplified view of the extracted circuit highlighting gene-related features. The circuit indicates strong contributions from token features corresponding to endothelial-related genes such as VWF, PTPRB, and SPARCL1.

Figure 5: Circuit extraction for endothelial cell classification. (a) Detailed extracted circuit for feature 3353. (b) Simplified circuit emphasizing gene-related features (e.g., VWF, PTPRB, SPARCL1).

While the extracted circuit contains many activated features, many correspond to tokens in the text prompt rather than gene names. Focusing on features activated by gene name tokens, we identified particularly strong activations for:

- VWF (von Willebrand factor): a canonical endothelial marker localized to Weibel–Palade bodies [16].
- PTPRB (VE-PTP): an endothelial-enriched receptor-type tyrosine phosphatase that regulates junctional integrity and TIE2 signaling [5].
- SPARCL1 (hevin): highly expressed in quiescent endothelial cells; contributes to vessel stability and barrier maintenance [13].

These genes are all closely associated with endothelial cell biology, suggesting that the extracted circuit captures biologically meaningful patterns. However, the circuit remains large and complex, with many features difficult to interpret biologically. This highlights the need for more refined circuit extraction methods and feature interpretation techniques in future work.

5 Related Work

While mechanistic interpretability of large-scale models including LLMs has attracted significant attention [6, 10, 9], the field remains in its early exploratory stages. Particularly, applications of mechanistic interpretability techniques from natural language processing to bioinformatics models such as single-cell analysis models are still limited. Here we summarize the relationship between our work and these pioneering studies.

Schuster’s scFeatureLens [14] and work by Claye et al. [3] have applied sparse autoencoders to scFMs such as Geneformer [15] and scGPT [4], providing frameworks to mechanistically interpret SAE features as biological concepts. Our research extends this line of work by utilizing transcoders, an advanced variant of SAEs, to extract internal decision circuits from scFMs and demonstrate their correspondence with biological concepts. The frameworks developed in these prior studies could potentially be applied to individual transcoder features, suggesting valuable directions for future research.

Additionally, mechanistic interpretability techniques have been applied to models that directly process genome sequences. For instance, Brixi et al. developed Evo 2 [2], a genomic foundation model, and as part of their research incorporated SAE analysis to investigate the model’s internal representations, revealing that it recognizes biologically important sequence patterns such as intron-exon boundaries. These studies collectively demonstrate the growing potential of mechanistic interpretability methods in understanding biological foundation models.

6 Conclusion and Future Work

In this work, we demonstrated that applying transcoders to scFMs enables the extraction of biologically interpretable features and internal decision-making circuits. To our knowledge, this is the first application of transcoders and circuit tracing to mechanistic interpretability of scFMs, opening new avenues for interpretability research in single-cell analysis models.

However, this work has several limitations that present opportunities for future research. First, the biological interpretation of extracted internal circuits was performed manually, which is time-consuming and potentially subjective. Future work should develop automated interpretation methods that can systematically map transcoder features to biological concepts. Second, the choice of training dataset significantly impacts the features learned by transcoders. While we used Heart Cell Atlas v2, exploring other datasets could reveal more general features and circuits applicable across different cell types and biological contexts.

Future research directions include developing novel methods to further enhance scFM interpretability and applying these techniques to discover new biological insights. The improvement of scFM interpretability holds significant potential for advancing single-cell biology, as understanding how these models make decisions could reveal previously unknown biological relationships and mechanisms.

We anticipate that the field of scFM interpretability will continue to evolve, bringing new insights to single-cell analysis and contributing to our understanding of cellular biology at unprecedented resolution. As scFMs become increasingly integrated into biological research workflows, ensuring their interpretability will be crucial for building trust and enabling scientific discovery.

References

- [1] Stella Biderman, Hailey Schoelkopf, Quentin Anthony, Herbie Bradley, Kyle O’Brien, Eric Hallahan, Mohammad Afshar Khan, Shivanshu Purohit, USVSN Sai Prashanth, Edward Raff, Aviya Skowron, Lintang Sutawika, and Oskar van der Wal. Pythia: A suite for analyzing large language models across training and scaling. In *Proceedings of the 40th International Conference on Machine Learning*, volume 202 of *Proceedings of Machine Learning Research*. PMLR, 2023.
- [2] Garyk Brixi, Matthew G. Durrant, Jerome Ku, Michael Poli, Greg Brockman, Daniel Chang, Gabriel A. Gonzalez, Samuel H. King, David B. Li, Aditi T. Merchant, Mohsen Naghipourfar, Eric Nguyen, Chiara Ricci-Tam, David W. Romero, Gwanggyu Sun, Ali Taghibakshi, Anton Vorontsov, Brandon Yang, Myra Deng, Liv Gorton, Nam Nguyen, Nicholas K. Wang, Etowah

- Adams, Stephen A. Baccus, Steven Dillmann, Stefano Ermon, Daniel Guo, Rajesh Ilango, Ken Janik, Amy X. Lu, Reshma Mehta, Mohammad R.K. Mofrad, Madelena Y. Ng, Jaspreet Pannu, Christopher Ré, Jonathan C. Schmok, John St. John, Jeremy Sullivan, Kevin Zhu, Greg Zynda, Daniel Balsam, Patrick Collison, Anthony B. Costa, Tina Hernandez-Boussard, Eric Ho, Ming-Yu Liu, Thomas McGrath, Kimberly Powell, Dave P. Burke, Hani Goodarzi, Patrick D. Hsu, and Brian L. Hie. Genome modeling and design across all domains of life with evo 2. *bioRxiv*, 2025.
- [3] Charlotte Claye, Pierre Marschall, Wassila Ouerdane, Céline Hudelot, and Julien Duquesne. A framework to extract and interpret biological concepts from scrnaseq generative foundation models. In *ICML 2025 Generative AI and Biology (GenBio) Workshop*.
- [4] Haotian Cui, Chloe Wang, Hassaan Maan, Kuan Pang, Fengning Luo, Nan Duan, and Bo Wang. scgpt: toward building a foundation model for single-cell multi-omics using generative ai. *Nature Methods*, 21(8):1470–1480, February 2024.
- [5] Hannes C. A. Drexler and others. Vascular endothelial receptor tyrosine phosphatase: Identification of novel substrates related to junctions and a ternary complex with ephb4 and tie2. *Molecular & Cellular Proteomics*, 18(10):2058–2077, 2019.
- [6] Jacob Dunefsky, Philippe Chlenski, and Neel Nanda. Transcoders find interpretable llm feature circuits. In *Proceedings of the 38th International Conference on Neural Information Processing Systems, NIPS '24*, Red Hook, NY, USA, 2025. Curran Associates Inc.
- [7] Nelson Elhage, Tristan Hume, Catherine Olsson, Nicholas Schiefer, Tom Henighan, Shauna Kravec, Zac Hatfield-Dodds, Robert Lasenby, Dawn Drain, Carol Chen, Roger Grosse, Sam McCandlish, Jared Kaplan, Dario Amodei, Martin Wattenberg, and Christopher Olah. Toy models of superposition. *arXiv preprint arXiv:2209.10652*, 2022.
- [8] Nelson Elhage, Neel Nanda, Catherine Olsson, Tom Henighan, Nicholas Joseph, Ben Mann, Amanda Askell, Yuntao Bai, Anna Chen, Tom Conerly, Nova DasSarma, Dawn Drain, Deep Ganguli, Zac Hatfield-Dodds, Danny Hernandez, Andy Jones, Jackson Kernion, Liane Lovitt, Kamal Ndousse, Dario Amodei, Tom Brown, Jack Clark, Jared Kaplan, Sam McCandlish, and Chris Olah. A mathematical framework for transformer circuits. *Transformer Circuits Thread*, 2021. Accessed 2025-09-08.
- [9] Robert Huben, Hoagy Cunningham, Logan Riggs Smith, Aidan Ewart, and Lee Sharkey. Sparse autoencoders find highly interpretable features in language models. In *The Twelfth International Conference on Learning Representations*, 2024.
- [10] Harish Kamath, Emmanuel Ameisen, Isaac Kauvar, Rodrigo Luger, Wes Gurnee, Adam Pearce, Sam Zimmerman, Joshua Batson, Thomas Conerly, Chris Olah, and Jack Lindsey. Tracing attention computation: Attention connects features, and features direct attention. *Transformer Circuits Thread*, 2025.
- [11] Kazumasa Kanemaru, James Cranley, Daniele Muraro, Antonio M A Miranda, Siew Yen Ho, Anna Wilbrey-Clark, Jan Patrick Pett, Krzysztof Polanski, Laura Richardson, Monika Litvinukova, Natsuhiko Kumasaka, Yue Qin, Zuzanna Jablonska, Claudia I Semprich, Lukas Mach, Monika Dabrowska, Nathan Richoz, Liam Bolt, Lira Mamanova, Rakesh Lal Kapuge, Sam N Barnett, Shani Perera, Carlos Talavera-López, Ilaria Mulas, Krishnaa T Mahbubani, Liz Tuck, Lu Wang, Margaret M Huang, Martin Prete, Sophie Pritchard, John Dark, Kourosh Saeb-Parsy, Minal Patel, Menna R Clatworthy, Norbert Hübner, Rasheda A Chowdhury, Michela Nosedà, and Sarah A Teichmann. Spatially resolved multiomics of human cardiac niches. *Nature*, 619(7971):801–810, July 2023.
- [12] Daniel Levine, Syed A Rizvi, Sacha Lévy, Nazreen Pallikkavaliyaveetil, David Zhang, Xingyu Chen, Sina Ghadermarzi, Ruiming Wu, Zihe Zheng, Ivan Vrkcic, Anna Zhong, Daphne Raskin, Insu Han, Antonio Henrique De Oliveira Fonseca, Josue Ortega Caro, Amin Karbasi, Rahul Madhav Dhodapkar, and David Van Dijk. Cell2sentence: Teaching large language models the language of biology. In *Proceedings of the 41st International Conference on Machine Learning*, volume 235 of *Proceedings of Machine Learning Research*, pages 27299–27325. PMLR, 2024.

- [13] Daniela Regensburger and others. Matricellular protein sparcl1 regulates blood vessel integrity and antagonizes inflammatory bowel disease. *Inflammatory Bowel Diseases*, 27(9):1491–1502, 2021.
- [14] Viktoria Schuster. Can sparse autoencoders make sense of gene expression latent variable models?, 2025.
- [15] Christina V. Theodoris, Ling Xiao, Anant Chopra, Mark D. Chaffin, Zeina R. Al Sayed, Matthew C. Hill, Helene Mantineo, Elizabeth M. Brydon, Zexian Zeng, X. Shirley Liu, and Patrick T. Ellinor. Transfer learning enables predictions in network biology. *Nature*, 618(7965):616–624, May 2023.
- [16] Karine M. Valentijn, J. Evan Sadler, Jack A. Valentijn, Jan Voorberg, and Jeroen Eikenboom. Functional architecture of weibel-palade bodies. *Blood*, 117(19):5033–5043, 2011.
- [17] van Dijk Lab. vandijklab/c2s-pythia-410m-cell-type-prediction. Hugging Face, 2025. Model card. Trained on ~57M single cells from CellxGene and HCA. Accessed 2025-09-08.